Nanoscale Electrochemical Studies: How Can We Use the Atomic Switch

Ilia Valov, Tsuyoshi Hasegawa, Tohru Tsuruoka, Rainer Waser, and Masakazu Aono

Abstract Scanning tunnelling microscopy (STM) and in particular the Atomic Switch concept provides a unique opportunity for site invariant, atomically resolved studies on the electrochemical reaction kinetics, combined with close monitoring of the surface morphology. This approach can be applied on particular active or defect sites, but also to larger surface areas, where electrochemically induced changes on the surface states and nanocluster dynamics are monitored by current-voltage (*I*-*V*) spectroscopy and/or current-displacement (*I*-*z*) spectroscopy.

The redox reaction kinetics of areas or sites with different electrocatalytic activity can be distinguished and independently characterized. By modification of the Buttler-Volmer equation, we use switching time as a kinetic parameter instead of current density, where this approach is independent on the electronic partial conductivity.

Thus, the Atomic Switch concept allows for redox kinetics studies with highest lateral, mass and charge resolution.

1 Introduction

Since its introduction and invention by Binnig and Rohrer [1, 2], scanning tunnelling microscope (STM) has been used for characterization and manipulation of electronically conductive surfaces providing unique opportunity for achieving atomic lateral resolution and precision [3–5]. STM is now an inevitable tool for high resolution in situ and ex situ studies in the fields such as surface science and (electro)catalysis. More recent developments have transferred this typically UHV technique to liquids, establishing the electrochemical STM [6, 7]. In most of its applications STM is used as a non-invasive tool for observation and/or characterization e.g. to image

---

I. Valov (✉) · R. Waser
Research Centre Jülich, Electronic Materials (PGI-7), Jülich, Germany
e-mail: i.valov@fz-juelich.de

T. Hasegawa · T. Tsuruoka · M. Aono
International Center for Materials Nanoarchitectonics (MANA), National Institute for Materials Science (NIMS), Tsukuba, Ibaraki, Japan

M. Aono (ed.), *Atomic Switch*, Advances in Atom and Single Molecule Machines,
https://doi.org/10.1007/978-3-030-34875-5_5

adsorption/desorption processes, structural and morphological evolutions, reconstruction of surfaces, changes in the electronic structure, etc. In two particular situations STM can also play the active role—atomic/cluster manipulations and the Atomic Switch. In the first case due to physical interactions and local heating generated between tip and substrate single (or group of) atoms can be removed/added and/or dragged on surfaces [5]. This technique has been further developed for nanostructuring i.e. STM lithography [8–10].

The Atomic Switch is the second and maybe the latest development in applications of STM. It has been invented by Terabe et al. and uses STM for inducing electrochemical transformations at surfaces, related with mass and charge transfer [11–13]. This technique is applied in the information technology for storing information and performing neuromorphic operations [14, 15].

A limiting factor for the applications of STM is the requirement for the samples to be electronically conductive. Thus, samples with insufficient electronic conductivity e.g. insulating oxides and purely ionic solid electrolytes are in principle not accessible by this technique. To avoid the restriction, several different approaches have been used. For example, insulating oxides can be reduced prior to STM experiments. Reduction can be achieved either by variation of the deposition conditions, or by annealing in reducing atmosphere. Alternatively, oxides can also be deposited very thin (few monolayers) or can be doped with foreign elements in order to increase their electronic conductivity to a sufficient level, however, without changing their structure. Many examples can be found using various oxides such as NiO, $SrTiO_3$, TiO_2, BaO, ZnO, Nb-STO, CeO_2 etc. but also for super ionic conductors [16–22].

In this chapter the use of the STM in electrochemical studies in the role of an active electrode will be demonstrated and discussed. Based on the Atomic Switch approach and also using it in combination with the other STM modes this technique provides the opportunity for site-invariant electrochemical studies with highest lateral, mass and charge resolution, using time as critical kinetic parameter. Theoretical discussion and particular examples will highlight this application.

2 (Sub-)Nanoscale Electrochemical Studies

Electrochemical studies at the nano- and sub-nanoscale are essential for mechanistic understandings of processes occurring in variety of applications within the fields of energy conversion and storage, sensors, (electro)catalysis, smart devices, nanoelectronics and information technology [23]. The small dimensions of electrodes and solid electrolytes and related small amounts of exchanged mass and charge challenge the sensitivity of the modern equipment. In addition, electrochemical experiments in nanoscale cells are accompanied by extreme conditions: Applying voltages even in the lower range of up to 1 V, corresponds to e.g. electric fields in the range of 10^7–10^8 V m^{-1} and current densities varying between $j \sim (10^4–10^9)$ A cm^{-2}. Moreover, non-trivial effects can appear, deviating from expectations and theories formulated for macroscopic samples. Thus, even insulating thin films of materials such as Ta_2O_5, HfO_2, SiO_2 etc. turn at nanoscale from high-k materials with insulating macroscopic properties into ionic or mixed ionic-electronic electrolytes at the nanoscale, blurring borders of macroscopic definitions for insulators, semiconductors and electrolytes [24].

The development of the field of nanoelectrochemistry has been especially accelerated by re-discovering the resistive switching memories and their applications not only as non-volatile memory but as building units for neuromorphic applications, alternative logic operations and beyond von Neumann computing [25, 26]. One of the reasons for this acceleration is the focus of both academia and industrial interest on the nanoscale processes. In other areas where electrochemistry plays an inevitable role such as energy conversion and storage or catalysis, industrial research and development targets typically middle and large scale applications, whereas academia aims microscopic understandings. In contrast, in the case of resistive switching memoires (and the Atomic Switch as a part of it) the interest and efforts of both academia and industry are concentrated on research and development of devices, cells and structures with lowest possible size, fastest kinetics, and highest scalability. This joint interest is especially productive and pushes forward the equipment development, fundamental research and technology/applications.

In that sense the Atomic Switch is used not only for information processing and storage, but can be a powerful tool for fundamental research of nanoscale electrochemical processes with highest precision.

3 Using the Atomic Switch

As any STM based technique, the Atomic Switch in generally can work only with materials providing a sufficient electronic conductivity. In a macroscopic sense solid materials (excluding metals) can be categorised as insulators, semiconductors/mixed ionic-electronic conductors and ionic conductors. As discussed above after appropriate treatment such as doping, annealing etc., most solid thin films can be used for STM studies. An example illustrating some of these materials related to the use of Atomic Switch is shown in Fig. 1.

Metals and highly doped semiconductors are usual materials choice for STM studies. However, within the Atomic Switch concept also ionic conductors and even materials considered macroscopic insulators can be modified in a way to become suitable for this technique without significantly changing their ionic transport characteristics and preserving their crystallographic structure.

For example $RbAg_4I_5$ is a superionic solid conductor with the highest reported room temperature ionic (Ag^+) conductivity, being measured in the order of 0.1 Ω^{-1} cm^{-1} [27, 28]. It provides a very suitable model system for studies on kinetics of electrode processes in solids. However, the low electronic conductivity of this material, suppressing the quantum mechanical tunnelling, is in principal not supporting STM studies. A way to avoid this restriction is using a doping approach, selectively increasing the electronic conductivity, without influencing the Ag^+ partial conductivity. It has been shown that small amount of Fe (0.1 at.%) introduced in $RbAg_4I_5$ are able to

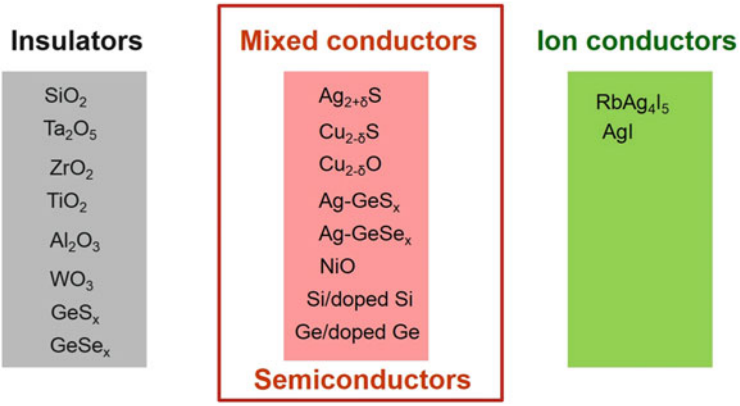

Fig. 1 Macroscopic classification of materials/compounds in respect their transport properties. The column in the middle shows materials that can be commonly used for STM studies. The other classes of materials require particular modifications to become suitable for Atomic Switch experiments

increase the electronic conductivity by orders of magnitude. In the same time the material remains superionic conductor with an ionic transference number of $t_{\mathrm{ion}} > 0.99$. Thus, the crystallographic structure and the superionic properties are preserved, but the electronic conductivity in the order of $\sigma_e = (10^{-2} - 10^{-3})\sigma_{\mathrm{ion}}$ was sufficient to enable STM imaging and experiments [21]. This approach has allowed to use the full functionalities of the STM on $RbAg_4I_5$ thin films, including imaging, *I*-*z* spectroscopy and Atomic Switch experiments.

Different approach has been used with oxides such as Ta_2O_5, HfO_2 and TiO_2. In a macroscopic sense they are high-k materials at room temperature and per definition not suitable for STM. In order to use STM on these materials the thickness of the studied layers should be reduced down to 3–5 nm and they should be annealed in vacuum in order to ensure some level of reduction, without reaching the level of decomposition. After such treatment the samples were able to be studied by scanning tunnelling microscope using all its analytical modes [29].

Thus, even “non-classical” materials such as insulators and purely ionic conductors can be modified in a way that enables Atomic Switch and in general STM studies.

4 The Atomic Switch as a Fundamental Approach for Electrochemical Studies

The atomic switch configuration is providing a unique opportunity to perform electrochemical studies with highest precision, lateral, mass and charge resolution. It combines both the technical advantages of the STM (imaging, morphology and electronic changes, *I*-*z* spectroscopy, STS spectroscopy) and the possibility to modify parameters not accessible by any other technique (e.g. by variation of the tunnelling distance). The STM tip can be also effectively used as an active electrode inducing electrochemical redox reactions at the surface of the solid electrolyte. Based on this new approach the reaction kinetics of several materials such as $RbAg_4I_5$, Ag_2S, Cu_2S, TaO_2, HfO_2 and TiO_2 has been studied [21, 29–32].

4.1 Theoretical Considerations

4.1.1 Imaging and Electrochemical Reactions

On a first place STM can be used to image the surface of the solid film and precisely (with atomic resolution) select the position for applying voltage and studying particular process(es).

For studies on macroscopic samples, the evaluated properties of surfaces are averaged and the main efforts are focused on the preparation of an ideal, defect free surface. Even mono-crystalline surfaces are showing microscopic defects, possible dislocations, missing atoms, monoatomic steps, etc., being energetically not equivalent, thus predetermining different local reaction kinetics. In that sense, STM is providing the unique opportunity to find and select defect-free position or particular defect site and perform locally electrochemical studies on it, without influencing and/or gathering information from neighbouring domains.

The sensitivity of the STM towards surface morphology inhomogeneity allows to follow the formation and dissolution of small number of atoms (even single atoms), providing an important advantage to observe finest changes induced at the surface. This sensitivity is determined by the exponential dependence of the tunnelling current on the tip-sample distance. The tunnelling current I_{tunnel} is given by the equation:

$$I_{\text{tunnel}} \sim e^{-2z\sqrt{\frac{2m_e}{(h/2\pi)^2}\Phi}} \tag{1}$$

where z is the width of the energy barrier, m_e is the effective mass of the electron, h is the Planck constant and Φ is the work function (representing the height of the tunnelling barrier). In the case of STM, the distance between tip and sample surface is corresponding to the width of the energy barrier z. Therefore, even very small changes in the distance z e.g. formation of a new atom beneath the tip can be easily detected by the increased tunnelling current.

In case of purely electronic conducting sample surfaces e.g. metals, changes in the surface morphology can appear (or can be induced) only at sufficiently high voltages due to the physical in nature tip-sample interactions. However, if we have an ionic or mixed ionic-electronic conductor also electrochemical redox reactions can be induced, that leads to formation of a new phase. In that respect the main

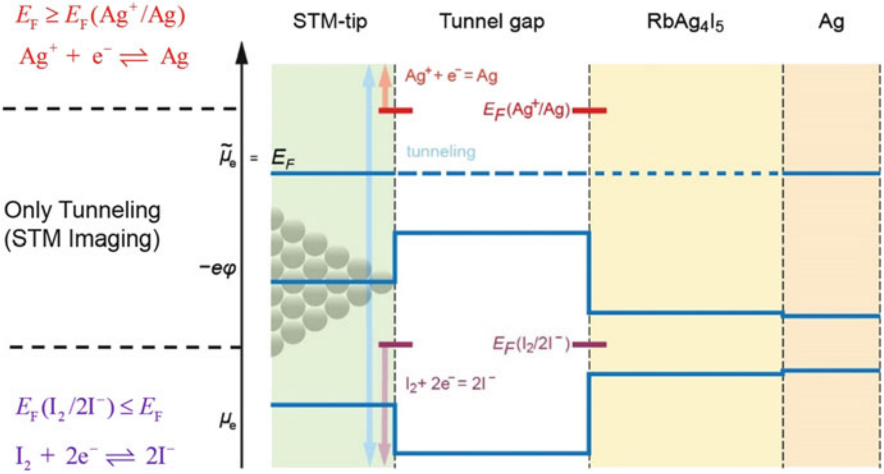

Fig. 2 Atomic switch (STM) configuration and energy level positions of the half-cell redox reactions at equilibrium state. The electrochemical potential of electrons $\tilde{\mu}_e$ is given by $\tilde{\mu}_e = \mu_e - ze\varphi$ (μ_e is their chemical potential and φ is the electric potential) and corresponds to their Fermi energy

question that appears is at which energetic conditions e.g. applied voltage, such reactions will be induced. Figure 2 is visualizing these conditions assuming constant temperature.

At equilibrium no voltage is applied and no driving force for electrochemical reactions is present. Approaching a tunnelling distance, the Fermi level of electrons of the STM tip and the sample, or in terms of thermodynamics their electrochemical potentials $\tilde{\mu}_e$(tip), $\tilde{\mu}_e$(Ag), equilibrate and the condition E_F(tip) = E_F(Ag) or, respectively, $\tilde{\mu}_e(\text{tip}) = \tilde{\mu}_e(\text{Ag})$ is fulfilled presuming no net current flow (at zero voltage). The main potential drop is concentrated between the STM tip and $RbAg_4I_5$ surface.

An applied voltage shifts the Fermi level of the STM tip relative to the sample ($\Delta E_F(\text{tip}) = -e\Delta\varphi$) and an effective tunnelling current is induced. Electrons coming at the $RbAg_4I_5$ surface with an energy lower than the Fermi energy of the redox reaction:

$$Ag^+ + e^- \rightleftharpoons Ag \tag{2}$$

i.e., $E_F < E_F(Ag^+/Ag)$ can only tunnel but cannot contribute to the electrochemical reaction.

After exceeding the energy level of $E_F > E_F(Ag^+/Ag)$ the tunnel electrons can overcome the energy barrier for the Ag^+/Ag redox reaction and Ag atoms will be formed at the electrolyte surface.

At the same moment in order to keep the electroneutrality within the solid electrolyte at the $RbAg_4I_5/Ag$ interface, an equal amount of Ag (from bottom electrode) will be oxidized to Ag^+ entering the $RbAg_4I_5$.

Thus, at $E_F < E_F(Ag^+/Ag)$ one can perform STM imaging and at $E_F > E_F(Ag^+/Ag)$—electrochemical measurements of the reaction kinetics.

Same discussion applies to the other half-cell reaction i.e.:

$$I_2 + \ 2e^- \rightleftharpoons 2I^- \tag{3}$$

Applying a sufficiently positive voltage to the tip will result in oxidation of I^- ions with formation of iodine.

Thus, the general condition for STM imaging without inducing electrochemical reactions is given by:

$$E_F(I_2/2I^-) < E_F < E_F(Ag^+/Ag) \tag{4}$$

For higher, respectively lower Fermi levels electrochemical reactions of reduction of Ag^+ or oxidation of I^- will be induced at the bare surface.

The Atomic Switch approach combined with scanning tunnelling spectroscopy (STS) and current-displacement (*I*-*z*) spectroscopy and imaging provides a unique opportunity for studying site-invariant electrochemical processes with highest possible resolution. It also allows to observe in situ or ex situ the stability and the dynamics of the formed atomic clusters and relate them to the electrochemical characteristics.

4.1.2 Using Time as a Kinetic Parameter

The methods used for studying kinetics of electrochemical electrode processes can be formally divided into stationary (or steady-state), dynamical and quasi-stationary (e.g. impedance spectroscopy) methods. To evaluate the reaction kinetics a precise knowledge on the partial ionic current is essential. Determining the partial ionic current (or the ionic transference number) is often a main challenge in electrochemistry. This especially applies to nanoscale systems. At small dimensions, structure and properties deviate from the expected macroscopically defined quantities and effects such as field assisted migration, leakage electronic currents and possibility for electron tunnelling through the electrolyte should be taken into account. In fact, the main contribution to the total current is the electronic partial current. Additionally, in case of field assisted migration (exponential dependence of the ion velocity from electric field and particle charge) the transference number can vary depending on the magnitude of the applied voltage. Thus, in these systems there is a principle difficulty to determine the ionic transference number and therefore to evaluate the Faraday reaction kinetics. One possible solution of this problem is using the Atomic Switch approach and introducing time (instead of current) as critical kinetic parameter. As an example can be considered the Butler-Volmer equation, describing the current density (j) – voltage ($\Delta\varphi$) relation for charge transfer limited electrode processes. Its classical form is given by:

$$j = j_0\left[\exp\left(\frac{(1-\alpha)z_i e}{k_\mathrm{B}T}\Delta\varphi\right) - \exp\left(-\frac{\alpha z_i e}{k_\mathrm{B}T}\Delta\varphi\right)\right] \tag{5}$$

with j_0 being exchange current density, k_B—the Boltzmann constant, T—the temperature, e—the electron charge, z_i the number of exchanged electrons and α denoting the transfer coefficient for the cathodic process.

In this form Eq. (5) cannot be applied to STM studies or to studies in nanoscale systems due to the high uncertainty in determining the ionic transference number. However, the Atomic Switch approach allows to modify the equation replacing the current density by the parameter switching time (t_s). To illustrate the approach, first the principle way the Atomic Switch operates should be illustrated, as depicted in Fig. 3.

During step 1 the surface of the solid electrolyte is scanned/imaged at positive tip voltages (fulfilling condition 4) in order to select the position (or site) for the experiments. After this step is completed, a negative voltage is applied ensuring $E_\mathrm{F} > E_\mathrm{F}(\mathrm{Ag}^+/\mathrm{Ag})$. This is inducing an electrochemical reaction (reaction (2)) and a metallic nucleus is formed at the electrolyte surface. This nucleus continues to grow into direction of the STM tip and short circuits the tunnel gap. The moment that the nucleus (or filament) short circuits the tunnel gap is related to a rapid increase of the conductivity. The time for completing this process can be precisely detected by measuring the conductivity (current) reaching the value of $G_0 = 2e/h = 78\ \mu S$ (or resistance of 12.9 kΩ). Technically, the time resolution of the modern equipment is fully capable in detecting times within or even below picosecond range.

Thus, the critical parameter in the Atomic Switch approach is the time for formation of a quantum point contact between the tip and the metallic nucleus (step 4 in Fig. 3).

The current density j from Bulter-Volmer equation can be expressed and related to the switching time according to:

$$j = \frac{I}{A} = \frac{Q}{A \cdot t_s} \tag{6}$$

where I is the absolute current value, A is the electrode surface area (being for the time of experiment constant), Q is the total charge related to reaction (2) and t_s is the time for establishing the quantum point contact (the switching time). As we measure the switching time, the only unknown parameter is the charge Q i.e. the number of electrons that are used in reaction 2. Figure 4 shows how Q can be estimated in a good approximation.

The tip-to-sample distance is fixed prior to applying the voltage and in the typical case for $\mathrm{RbAg_4I_5}$ was set to 1 nm. To fill this gap (distance) a row of 4 Ag atoms are required. This means that $4e^-$ is the minimum number of charges. However, ordering atoms in a chain and keeping this configuration is physically unrealistic,

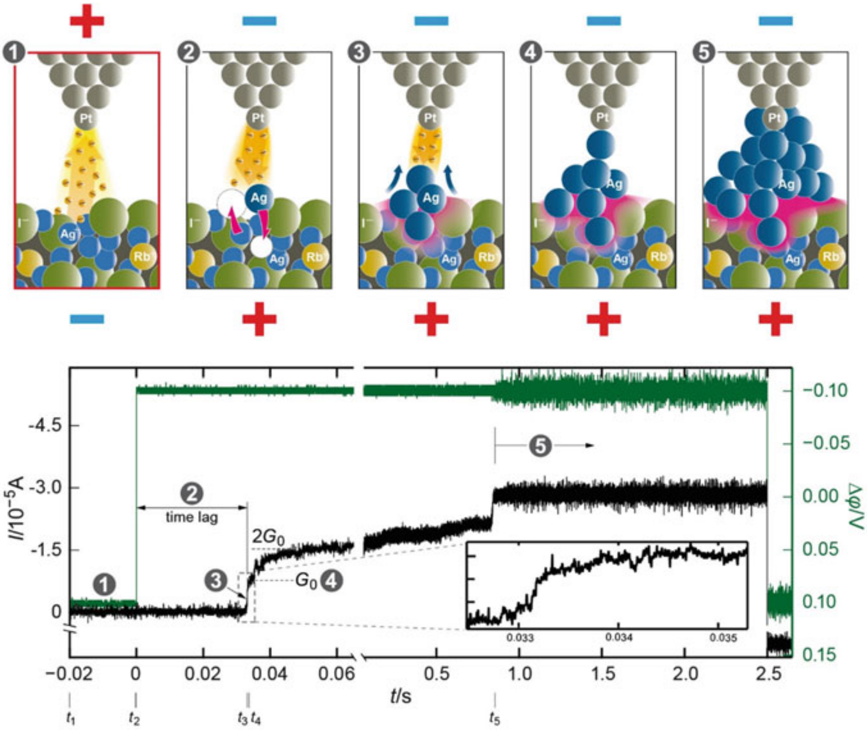

Fig. 3 Schematic presentation of physicochemical processes during Atomic Switch operation and the related current-time characteristics. Current-time dependence at applied voltage of –100 mV. The number (1–5) notation relates the five regions defined in the current-time characteristics to the microscopic model (upper part of the graph) for the sequence of individual steps during the switching. The inset shows the first quantum step at G_0. The sharpness of the current increase is determined by the rate of the filament growth. The figure is reproduced from [21]

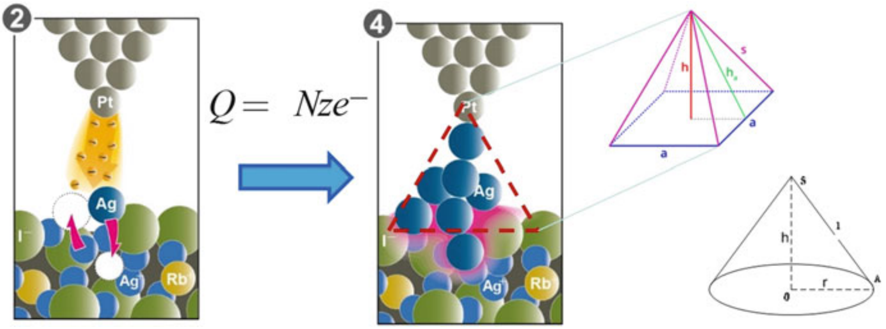

Fig. 4 Estimation of the charge used within the time for formation of quantum point contact

so we account for, that more atoms will be deposited within the switching time filling pyramidal or conical shape with a height of $h = 1$ nm. Taking into account the lateral distribution of the electric filed at the surface and the tunnelling electrons, the length of the base side-edge (or the radius) of this geometric form should be ~1 nm. This volume can be filled by 15–20 Ag atoms. Thus, the charge Q is given by the product of the number of atoms, the number of exchanged electrons per atom, and the electron charge. Now knowing Q we can substitute Eq. (6) into Eq. (5) and become the time-derived Butler-Volmer equation, which for the cathodic (reduction) process will be:

$$t_s = t_0 \cdot \exp\left(\frac{\alpha z_i e}{k_{\mathrm{B}} T} \Delta\varphi\right) \tag{7}$$

Thus, the Atomic Switch approach allows by measuring the switching time as a function of the applied voltage to extract the kinetic parameters of the electrode reaction in a manner as reliable as for classical approaches using the current-voltage relation. The resistance/conductivity of the tunnel gap will always change by short circuiting, irrespective on the particular material. It is also not disturbing the analysis whether the formed atoms remain stable at the surface or not. For volatile components one can expect (especially at higher temperatures) that after the initial moment of contact they will desorb. Even in this case the time-derived technique/analysis can be applied, as the only parameter we need is the time of achieving switching/contact. Thus, this type of studies can be applied to all materials with some ionic conductivity and being able to support electrochemical reactions.

4.1.3 Using STM Tip to Modify the Transfer Coefficient α

Using STM is allowing for another degree of freedom for tuning the experimental conditions during electrochemical experiments, inaccessible by any other technique. This is namely the possibility for variation of the transfer coefficient α. Figure 5 visualizes this by showing the potential energy—distance plot.

The charge transfer during electrode processes occurs within the electric double layer. This processes and the effects of the structure of the dense and diffusive double layer were intensively studied in in the classical electrochemistry in the last century e.g. [33, 34]. In the simplest case (provided no specific adsorption) the ion approaches the electrode surface and the distance has the thickness of the outer Helmholtz plane (OHP). At this position the electron transfer takes place, where the energy barrier also depends on the value of this distance. For classical electrochemical cell the thickness of the OHP depends only on the nature of the electrolyte (e.g. solvent, ions, etc.) and electrode material. In one of the earliest definitions the transfer coefficient was introduced as a symmetry factor [35] representing the geometrical position of the energy barrier maximum (for a charge transfer) within the OHP. In that sense the transfer coefficient α is fixed at constant other parameters.

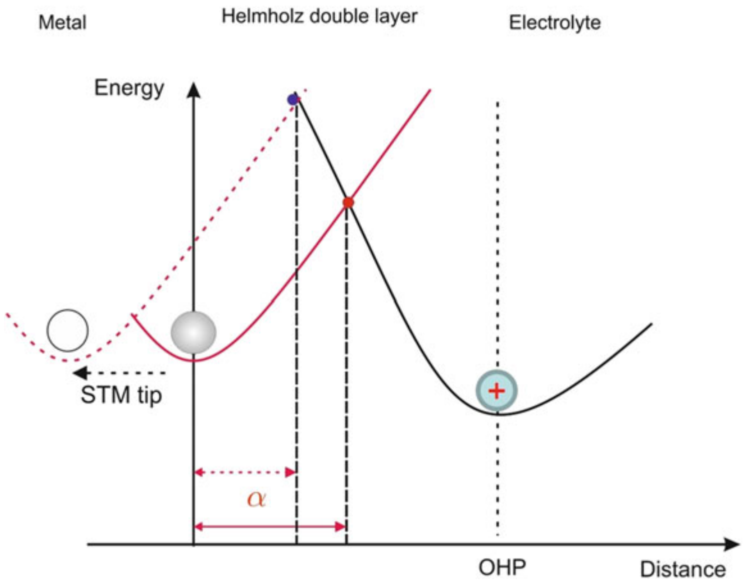

Fig. 5 Energy-distance plot for a charge transfer reaction. In the case of tip-to-sample distance can be varied (adjusted), using tunnelling current fulfilling the condition of Eq. (4)

In the case of Atomic Switch (STM) one can easily change the distance between the STM tip and the electrode surface and in this way to change the thickness of the OHP, and therefore the position of the energy barrier maximum i.e. the transfer coefficient. This provides the unique opportunity of studying the electrode processes tuning the transfer coefficient α, but keeping the same value of the applied potential and electrolyte composition.

4.2 Examples for Studying Electrochemical Processes Using the Atomic Switch

The Atomic Switch approach as described and discussed above, combined with other STM based techniques has been successfully applied for studies on electrochemical processes and reaction kinetics at solid electrolytes and oxides surfaces. These studies have demonstrated the power of this method and have provided information on the kinetics of different redox reactions.

4.2.1 Ag^+ Reduction at $RbAg_4I_5$ Surface

The kinetics of the cathodic reduction of Ag^+ (reaction 2) at the surface of $RbAg_4I_5$ was studied in details by the Atomic Switch technique. It has been found that the reaction 2 (i.e. condition $E_F > E_F(\mathrm{Ag}^+/\mathrm{Ag})$) starts at ~ –70 mV cathodic voltage. The current-time signal is shown in Fig. 3 at –100 mV applied bias. The time for establishing a quantum point contact (and related current increase) is shown in the zoomed window. In can be seen that for a certain period of time, after –100 mV were applied, the current remains low and constant and no increase was observed (step 2 in Fig. 3). This induction period (or time lag) can be explained only by a slow phase formation (nucleation) of the critical nucleus. In this way using the Atomic Switch approach we were also able to distinguish between different kinetic limitations, in this case that nucleation instead of charge transfer or ion diffusion is rate limiting.

Increasing the magnitude of the applied voltage resulted in qualitatively same current time responses, where only the induction time (time lag region) shortens. In this experiment, the applied voltage was varied between –100 and –600 mV and t_s has been recorded. The same experiments were repeated at different temperatures in order to determine the activation energy of the process. The results of the performed analysis are shown in Fig. 6.

As it can be seen in Fig. 6a the semi-logarithmic plot shows not a continuous but a discrete character showing two distinctive regions. At that point we have to account that approaching nano- and/or sub-nano dimensions the number of ions/atoms we exchange with the solid electrolyte is reduced below ~20. Thus, instead of the classical theory of nucleation we have applied the atomistic theory [36]. The nucleation equation was modified by substation with Eq. (6) as follows [21]:

$$t_s = t_0 \exp\left(\frac{(N_c + \alpha)e\Delta\varphi}{kT}\right) \tag{8}$$

where N_c is the number of the atoms constituting the critical nucleus.

Depending on the voltage range N_c has been determined to be 1 and 0, respectively, the transfer coefficient $\alpha = 0.2$ and the activation energy of the process was $\Delta G_a = {\sim}1$ eV.

Except determining the kinetic parameters of the reaction, we were able also to image Ag clusters and also to observe their life-time. Figure 7a–c shows STM images of formed clusters. The smallest stable cluster we were able to image is of a height of roughly 3 nm. We used also I-z to monitor smaller clusters and cluster dynamics. It has been observed that small nuclei are spontaneously dissolved after the applied voltage was removed (Fig. 7d), corresponding to unstable nucleus configuration. Applying higher voltages (currents) results in a stabilization of the clusters with a height of approximately 1 nm (Fig. 7e). Higher voltages (over 200 mV) and currents lead to stable nuclei of larger size (Fig. 7f).

Thus, we were able to determine the kinetic parameters and rate limiting step for $\mathrm{Ag}^+/\mathrm{Ag}$ redox reaction and also the conditions for stability of the deposited clusters.

Atomic Switch experiments discussing the switching time and mechanism and reaction kinetics have been also performed for mixed ionic-electronic solid electrolytes using Ag_2S and Cu_2S as model systems [30, 31]. In these experiment no

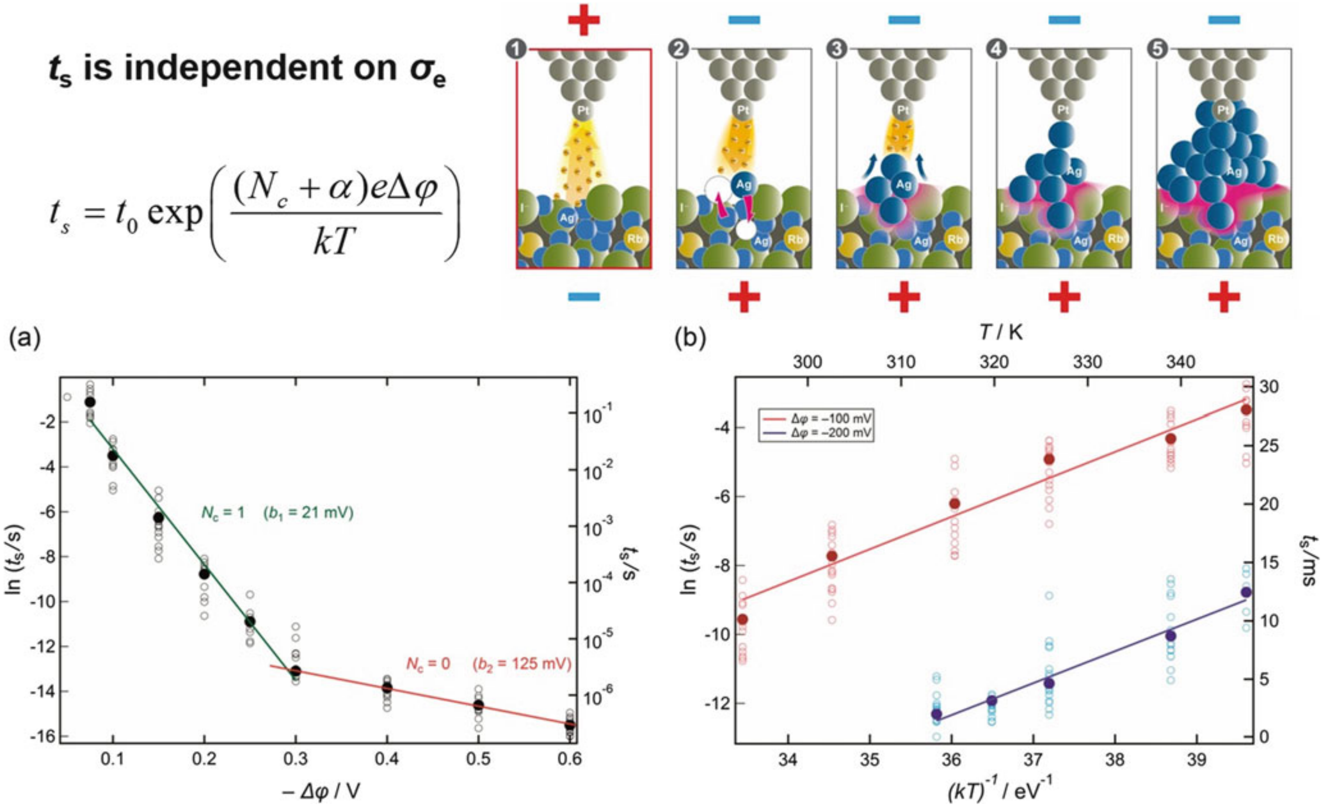

Fig. 6 Analysis of electrode kinetics of Ag^+ reduction at the $RbAg_4I_5$ surface. Plots of applied voltage vs. time (**a**) and Arrhenius type plot (**b**) are shown. The figure is modified from [21]

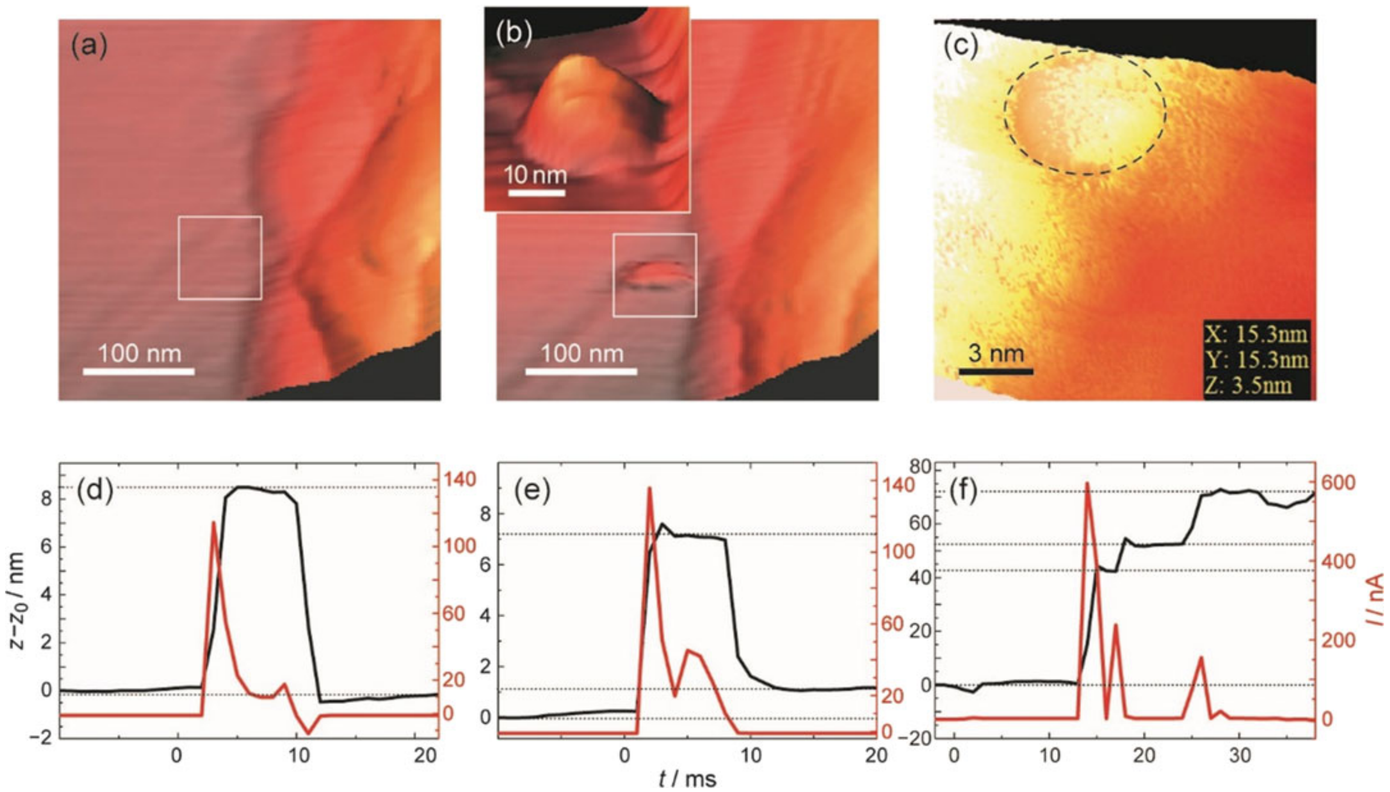

Fig. 7 STM images of electrochemically formed Ag clusters. (**a**) Before and (**b**) after the formation of the nucleus. (**c**) The smallest nucleus being able to be imaged within its stability time. (**d**–**f**) *I*-*z* spectroscopy showing different stages of growth and stability of Ag nuclei. The figure is reproduced from [21]

modification/doping of the thin film electrolytes was necessary, because the intrinsic electronic conductivity was sufficient for electron tunnelling.

These results have demonstrated the potential of the Atomic Switch (and STM in general) as powerful tool for studies of electrochemical processes with an ultimate lateral, mass and charge resolution.

4.2.2 Redox Processes on Oxides Studied by Atomic Switch

The concept of the Atomic Switch has been further developed and applied on oxides such as Ta_2O_5, HfO_2 and TiO_2. These samples have been adapted for Atomic Switch studies by annealing in vacuum in order to slightly increase their electronic conductivity. As discussed in the previous section the electronic conductivity is not influencing the kinetic measurements of the ionic redox reactions.

Applying different voltage polarities to the STM tip, it has been possible to distinguish between two different partial redox reactions, indicating that different ionic species are involved in the electrode reaction process. The system used for these experiments was $Ta_2O_{5\text{-}x}$ thin film deposited on 300 nm metallic Ta. As in the case of $RbAg_4I_5$ we firstly applied negative voltage to the tip and have observed formation of metallic nuclei at the oxide surface. We were also able to detect the formation of quantum point contacts for each of the experiments. Figure 8 shows STM images recorded after three consecutive switching events.

Using negative tip voltage we formed clusters of metallic Ta as also confirmed from the STS sweeps (sweep 3) performed immediately after the cluster formation. It shows a linear relation between voltage and current, thus evidencing for a metallic phase. The formed nucleus is however prone to re-oxidation and if one waits for ~15 min the metallic nucleus is covered by oxide scale (sweep 1 black curve) showing restored band gap. This surface oxide can be easily reduced back to metallic state (sweep 1 red curve).

Applying a positive bias to the tip results in a completely different electrical responses and images at the $Ta_2O_{5\text{-}x}$ surface. No formation of quantum point contact was observed at these conditions. The form and morphology of the modified areas were much broader and semiconducting instead of metallic properties were detected as evident from the STS sweeps, indicating that no metallic phase has been formed.

Based on these analysis it has been concluded that during the cathodic process (negative tip bias) the main reacting species are metal cations that are reduced to form metallic nuclei, whereas during the anodic process (positive tip bias) oxygen ions have been oxidized and oxygen has been released. Thus, depending on the applied voltage polarity different ionic species are undergoing electrochemical reaction at the interface.

Similar experiments were performed with other oxides such as $HfO_{2\text{-}x}$ and $TiO_{2\text{-}x}$ [32].

These conclusions were further supported and additional details on these processes were provided by using STM on larger surface areas on the oxide surfaces. Applying a negative voltage to the tip caused a reduction of the selected area. The

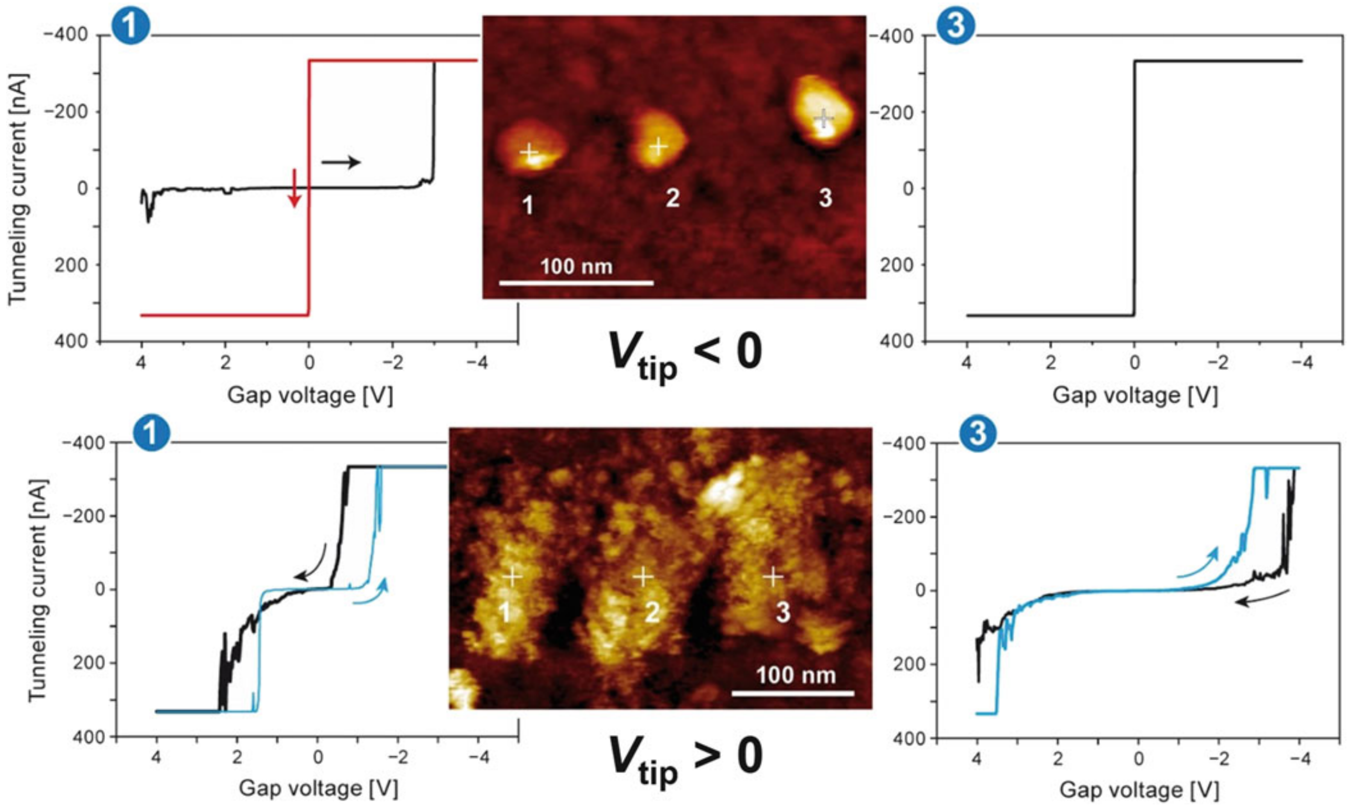

Fig. 8 Atomic switch experiments on Ta_2O_{5-x} surface using negative (upper image) and positive voltage polarity on the tip. Scanning tunnelling spectroscopy has been used to characterize the electronic structure of the modified surfaces. The figure is modified from [32]

reduced surface could be reversibly re-oxidized by applying a positive tip voltage. In Fig. 9 the recorded images for these experiment are presented.

The modified areas have been studied by ST spectroscopy to identify the changes in the electronic structure and conclude on the nature of induced modifications. As it can be seen from the *I*-*V* plot in Fig. 9 the reduced state shows purely metallic behaviour with liner relation between tunnelling current and applied voltage. After re-oxidation the metallic atoms are oxidized and the bandgap of the oxide was restored. Thus, we have confirmed that Ta-ions can be reduced at the surface of TaOx and reversible re-oxidized without inducing irreversible changes on the surface morphology.

Similar experiments have been performed by initially applying positive voltage to the STM tip. In this case the surface has been again modified but instead expected oxidation a clearly pronounced reduction of the selected area was detected. These reduction could be reversibly removed by applying a negative tip voltage. The STM images can be seen in Fig. 10.

The observed changes were explained by removing oxygen ($2O^{2-} - 4e^{-} = O_2$) from the Ta_2O_{5-x}, thus causing an effective reduction of the surface. An additional peak was observed close to the unoccupied states, indicating defect states in the band gap. Calculations on the hexagonal Ta_2O_5 structure revealed that occupied states mainly correspond to O 2p levels and unoccupied states to Ta 5d and 6s levels. Creating oxygen vacancies in the structure leads to an extra peak in LDOS close to the unoccupied states due to electron localization on Ta 5d and 6s states. The extra peak found in our experimental d*I*/d*V* data is consistent with this computational LDOS analysis on Ta_2O_5. The characteristic peak close to the unoccupied states and smaller band gap on LRS confirm resistive switching by an oxygen vacancy mechanism [29].

In these large scale experiments we were able also to distinguish that the predominance of one of the ionic species i.e. Ta^{x+}-cations or O^{2-}-anions in the redox reactions is strongly influenced by the stoichiometry of the oxide. Thus, more strongly reduced Ta_2O_{5-x} shows cation-type switching (as in Fig. 9), whereas less reduced Ta_2O_{5-y} ($y < x$) allows only anion-type switching. Therefore, it can be concluded that the level of non-stoichiometry also influences significantly the ionic transference numbers. These conclusions were supported by theoretical calculations showing the same trend.

Redox reactions, effects of polarity of the applied voltage and the influence of oxygen molecules have also been studied with purely electronic oxides e.g. $SrRuO_3$ that however, allow STM-tip induced ionic redox reactions. The electrical and structural properties of $SrRuO_3$ are very sensitive to the oxygen non-stoichiometry in the material and distinguishing between these effects is very challenging. The complex processes that were observed during anodic or respectively cathodic polarization were able to be resolved only by a combination of STM imaging, spectroscopy as well supported by PEEM and AFM analysis.

Under ultra-high vacuum conditions applying of positive tip bias resulted in irreversible modifications (reduction) of the surface. Two processes, different in nature, were able to explain these initial observations—(1) purely structural changes

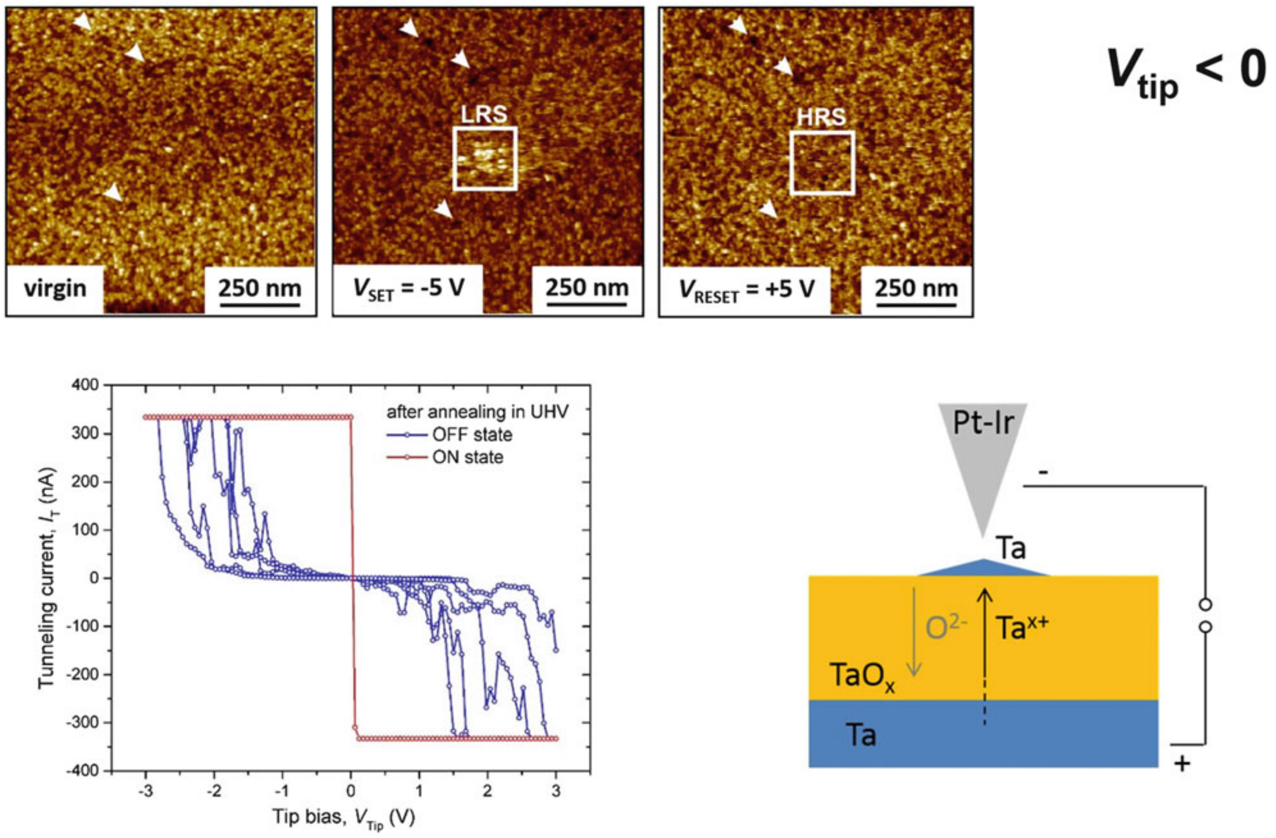

Fig. 9 STM experiment with electrochemical polarization causing reduction of the initial surface (left) at $V_{set} = -5$ V (middle) and re-oxidation at positive tip bias of $V_{reset} = 5$ V. The Ta_2O_5 film (deposited by RF sputtering on 100 nm metallic Ta) has been reduced in the vacuum chamber by annealing in vacuum at 300°C for 5 min in order to enable STM experiments. The figure is reproduced from [29]

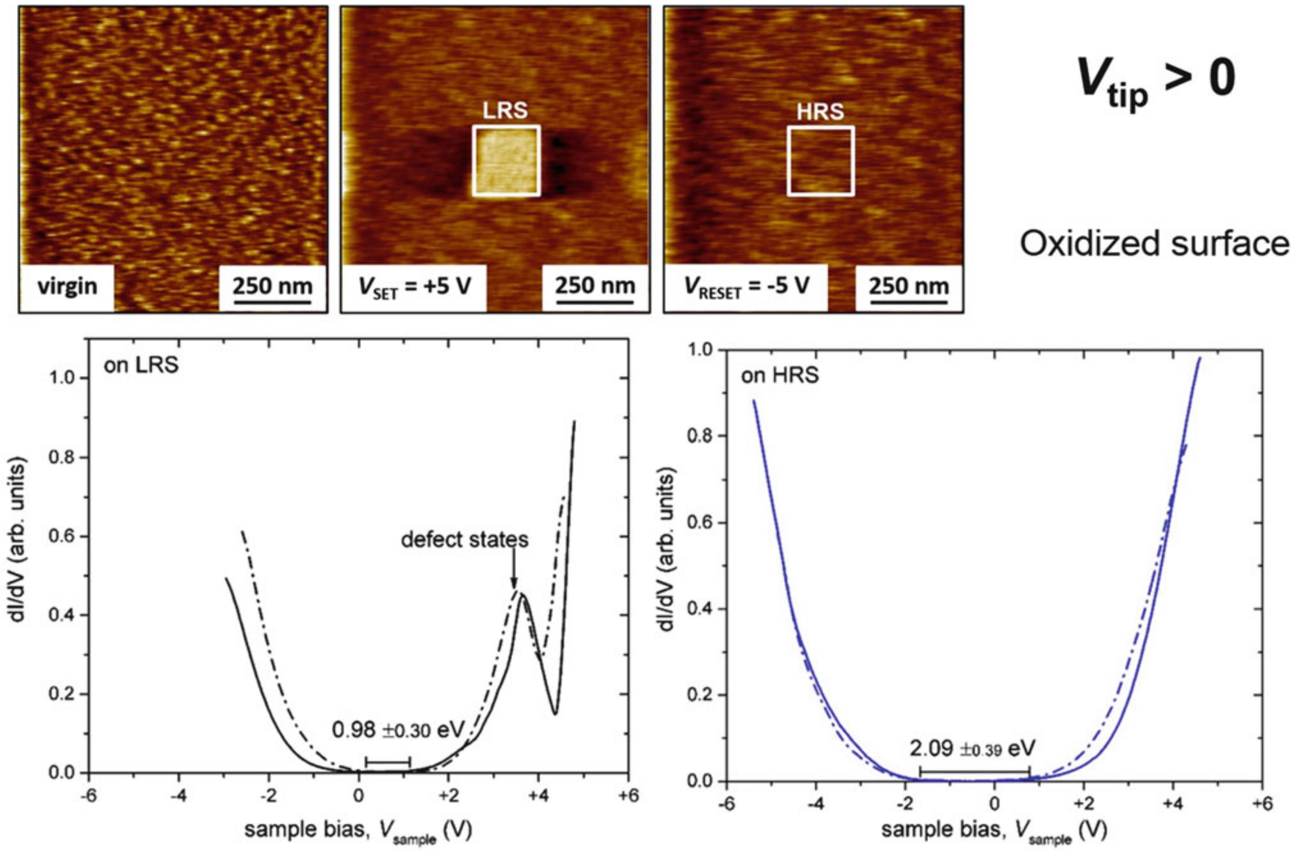

Fig. 10 STM experiment with electrochemical polarization causing reduction of the initial surface (left) at $V_{set} = 5$ V (middle) and re-oxidation at negative tip bias of $V_{reset} = -5$ V. The Ta_2O_5 film (deposited by RF sputtering on 100 nm metallic Ta) has been reduced in the vacuum chamber by annealing in vacuum at 300°C for 5 min in order to enable STM experiments. The figure is reproduced from [29]

within the $SrRuO_3$ or (2) redox reactions, related to change of stoichiometry. Both possibilities are related to loss of oxygen ions. To resolve this issue small amount of oxygen was introduced in the STM chamber. Without applied voltage no effect of O_2 has been observed. However, by applying a negative tip voltage it was possible to verify that the redox reactions related to change in stoichiometry but not decomposition (change of structure) induced from the STM tip were responsible for the observed behaviour. In presence of molecular oxygen the loss of oxygen ions within the oxide lattice could be completely reversed by applying negative tip bias, thus forming O^{2-} that is incorporated into the $SrRuO_{3-x}$ to restore the initial stoichiometry of $SrRuO_3$ [29]. Structural changes (being completely irreversible) were in addition safely excluded by PEEM/AFM analysis.

In contrary the cathodic changes caused by initial negative tip bias were relieved, trigged by internal self-induced process. $SrRuO_3$ is typically p-type conducting and of this reason enrichment with oxygen vacancies (positive relative charge in the sub-lattice) leads first to conditions of $p \sim n$ and further can lead to change to n-type conductivity. Applying negative tip voltage attracts the oxygen vacancies causing these changes. However, no oxygen ions are effectively lost and after removing the applied bias the vacancy concentration can relax and the initial profile is restored [29].

Thus, it was demonstrated that STM studies can be very powerful tool for inducing and studying electrode reactions on oxide interfaces, using materials of different composition and electronic/ionic properties.

5 Conclusions

The Atomic Switch approach is an alternative and powerful way to study electrochemical surface reactions with highest lateral, mass and charge resolution. In combination with classical STM modes it allows precise, site-invariant selection of the reaction location, avoiding statistical signal deviations averaged over properties of larger electrode surfaces. Instead of current, it uses the switching time (short circuiting the tunnel gap) as a critical kinetic parameter and is insensitive to the electronic partial conductivity of the materials. The variation of the tip-sample distance provides the unique opportunity to define and/or change the transfer coefficient of the charge transfer reactions, by keeping all other parameters constant.

The Atomic Switch can be used not only on electronically conducive materials but also on ionic solid electrolytes and even macroscopically insulating oxides after appropriate doping and/or treatment. The presented examples on difference classes of materials such as $RbAg_4I_5$, Ta_2O_5 and $SrRuO_3$ have demonstrated the ability of this method not only to allow to determine the kinetic parameters of a particular redox reaction but also to distinguish between different reacting species and rate limiting steps. This technique will be further developed for even atomically resolved experiments and expand the variety of studied materials and reactions.

References

1. Binnig, G., Rohrer, H.: Surf. Sci. **126**, 236 (1983)
2. Binnig, G., Rohrer, H.: Helv. Phys. A. **55**, 726 (1982)
3. Güntherodt, H.-J., Wiesendanger, R.: Scanning Tunneling Microscopy I: General Principles and Applications to Clean and Adsorbate-Cover Surfaces. Springer, Berlin (1994)
4. Wiesendanger, R.: Scanning Probe Microscopy and Spectroscopy: Methods and Applications. Cambridge University Press, Cambridge (1994)
5. Voigtländer, B.: Scanning Probe Microscopy. Springer, Berlin (2015)
6. Kolb, D.: Surf. Sci. **500**, 722 (2002)
7. Gentz, K., Wandelt, K.: Chimia. **66**, 44 (2012)
8. Garfunkel, E., Rudd, G., Novak, D., Wang, S., Ebert, G., Greenblatt, M., Gustafsson, T., Garofalini, S.: Science. **246**, 99 (1989)
9. Iwasaki, H., Yoshinobu, T., Sudoh, K.: Nanotechnology. **14**, R55 (2003)
10. Liu, Y., Zhang, J.: Physica B. **405**, 1890 (2010)
11. Terabe, K., Hasegaw, T., Nakayama, T., Aono, M.: Riken Rev. **37**, 7 (2001)
12. Terabe, K., Hasegawa, T., Nakayama, T., Aono, M.: Nature. **433**, 47 (2005)
13. Terabe, K., Nakayama, T., Hasegawa, T., Aono, M.: J. Appl. Phys. **91**, 10110 (2002)
14. Hasegawa, T., Terabe, K., Tsuruoka, T., Aono, M.: Adv. Mater. **24**, 252 (2012)
15. Ohno, T., Hasegawa, T., Tsuruoka, T., Terabe, K., Gimzewski, J.K., Aono, M.: Nat. Mater. **10**, 591 (2011)
16. Esch, F., Fabris, S., Zhou, L., Montini, T., Africh, C., Fornasiero, P., Comelli, G., Rosei, R.: Science. **309**, 752 (2005)
17. Diebold, U.: Appl. Phys. A Mater. Sci. Process. **76**, 681 (2003)
18. Setvin, M., Aschauer, U., Hulva, J., Simschitz, T., Daniel, B., Schmid, M., Selloni, A., Diebold, U.: J. Am. Chem. Soc. **138**, 9565 (2016)
19. Castell, M.R., Wincott, P.L., Condon, N.G., Muggelberg, C., Thornton, G., Dudarev, S.L., Sutton, A.P., Briggs, G.A.D.: Phys. Rev. B. **55**, 7859 (1997)
20. Castell, M.: Surf. Sci. **516**, 33 (2002)
21. Valov, I., Sapezanskaia, I., Nayak, A., Tsuruoka, T., Bredow, T., Hasegawa, T., Staikov, G., Aono, M., Waser, R.: Nat. Mater. **11**, 530 (2012)
22. Sterrer, M., Freund, H.: Surf. Interface Sci. **3**, 229–278 (2014). Volume 3: Properties
23. Valov, I., Lu, W.D.: Nanoscale. **8**, 13825–13827 (2016)
24. Valov, I., Lu, W.: Nanoscale. **8**, 13828 (2016)
25. Waser, R., Aono, M.: Nat. Mater. **6**, 833 (2007)
26. Valov, I.: ChemElectroChem. **1**, 26 (2014)
27. Bredikhin, S.I., Bondarev, V.N., Boris, A.V., Pikhitsa, P.V., Weppner, W.: Solid State Ionics. **81**, 19 (1995)
28. Scrosati, B.: J. Appl. Chem. Biotechnol. **21**, 223 (1971)
29. Moors, M., Adepalli, K.K., Lu, Q., Wedig, A., Bäumer, C., Skaja, K., Arndt, B., Tuller, H.L., Dittmann, R., Waser, R., Yildiz, B., Valov, I.: ACS Nano. **10**, 1481 (2016)
30. Nayak, A., Tamura, T., Tsuruoka, T., Terabe, K., Hosaka, S., Hasegawa, T., Aono, M.: J. Phys. Chem. Lett. **1**, 604 (2010)
31. Nayak, A., Tsuruoka, T., Terabe, K., Hasegawa, T., Aono, M.: Nanotechnology. **22**, 235201/1 (2011)
32. Wedig, A., Luebben, M., Cho, D.-Y., Moors, M., Skaja, K., Rana, V., Hasegawa, T., Adepalli, K., Yildiz, B., Waser, R., Valov, I.: Nat. Nanotechnol. **11**, 67 (2016)
33. Frumkin, A.N.: Z. Phys. Chem. **164A**, 121 (1933)
34. Delahay, P.: Double Layer and Electrode Kinetics. Wiley, New York (1965)
35. Erdey-Gruz, T., Volmer, M.: Zeitschrift für Physikalische Chemie A (Leipzig). **150A**, 203 (1930)
36. Milchev, A.: Nanoscale. **8**, 13867 (2016)